Thermochimica Acta xxx (2008) xxx–xxx

Contents lists available at ScienceDirect

Thermochimica Acta

journal homepage: www.elsevier.com/locate/tca

Thermodynamics and properties of nanophases☆

Bernhard Wunderlich[a,b,*]

[a] Department of Chemistry, University of Tennessee, Knoxville, TN 37996-1600, USA
[b] Chemical Sciences Division, Oak Ridge National Laboratory, Oak Ridge, TN 37831-6197, USA

ARTICLE INFO

Article history:
Available online xxx

Keywords:
Nanophase thermodynamics
Molecule type
Phase type
Phase size
Glass transition
Order–disorder transition
Nanophase
Microphase
Macrophase
Structure
Property

ABSTRACT

A large volume of today's research deals with nanophases of various types. The materials engineer, chemist, or physicist, however, when dealing with applications of nanophases is often unaware of the effect of the small size on structure and properties. The smallest nanophases reach the limit of phase definitions by approaching atomic dimensions. There, the required homogeneity of a phase is lost and undue property fluctuations destroy the usefulness of thermodynamic functions. In fact, it was not expected that a definite nanophase would exist below the size of a microphase. An effort is made in this review to identify macrophases, microphases, and nanophases. It is shown that nanophases should contain *no* bulk matter as defined by macrophases and also found in microphases. The structure and properties of nanophases, thus, must be different from macrophases *and* microphases. These changes may include different crystal and amorphous structures, and phase transitions of higher or of lower temperature. The phase properties are changing continuously when going from one surface to the opposite one. The discussion makes use of results from structure determination, calorimetry, molecular motion evaluations, and molecular dynamics simulations.

Published by Elsevier B.V.

1. Introduction

Feynman's brilliant popular science lecture at the 1959 annual meeting of the American Physical Society "Plenty of Room at the Bottom" [1] must be placed at the beginning of the enormous, present-day effort to understand the structure and properties of small particles of matter. He introduced the topic by stating: "In the year 2000, when they look back at this age, they will wonder why it was not until the year 1960 that anybody began seriously to move in this direction." Feynman pointed out that by enlarging the head of a pin (of diameter 1/16 in. = 1.6 mm) by a factor of 25,000, it would be the area of all pages in the Encyclopædia Britannica. Printing with the typical resolution of illustrations in books (120 dpi), makes one dot 8 nm across, or yields a dot of more than 1000 atoms. This seemed doable to Feynman and could even leave "plenty of room" for improvement (by pointing to the example of the size of information stored in a DNA molecule). When he discussed the way to assemble such small structures from the bottom up, molecule by molecule, or by manufacture from the top down, he speculated about the changes in properties when approaching very small dimensions: "I can hardly doubt that when we have some control of the arrangement of things on a small scale we will get an enormously greater range of possible properties that substances can have, and of different things that we can do."

How long did it take until this prophetic lecture caught on? Today, we can check the developments after 1960 by looking into the Chemical Abstracts (CAPLUS) and the National Library of Medicine (MEDLINE) and search electronically by using the SciFinder Scholar [2]. The first listing of *nanotechnology* was in a review of 1978 (Nanotechnology: Materials Processing with an Atomic or Molecular Size Working Unit—in Japanese, with five references) [3]. By early May 2008, this concept of nanotechnology had made it into over 500,000 publications [2]. The term, however, was already placed in 1974 into a frequently updated dictionary (described as "the art of manipulating materials on an atomic or molecular scale") [4].

The next most common term, *nanoparticles*, was first cited in 1976, describing pharmaceutical research [5]. Overall 125,000 entries are listed thereafter. The term made it into the dictionary by1983 [4]. *Nanocrystals*, with almost 60,000 entries in the literature, go back to 1973 and were mentioned in the genesis of minerals [6]. *Nanomaterials* were described first in 1991 in a discussion of precursors on consolidation into a ceramic coating or bulk material [7] and followed with about 7000 publications using the same term by 2008. The latter two, more specific terms did not make it into the dictionary by the beginning of the 21st century when research into the dimension of *nanometers* took off exponentially. The term

* Correspondence address: Department of Chemistry, University of Tennessee, Knoxville, TN 37996-1600, USA. Tel.: +1 865 675 4532.
E-mail address: Wunderlich@CharterTN.net.

0040-6031/$ – see front matter. Published by Elsevier B.V.
doi:10.1016/j.tca.2008.10.026

"nanometer" was entered already into the dictionary in 1963 for the benefit of the general reading public [4].

Finally, in the year 2000, the term *nanothermodynamics* was created by Hill [8], the well-known scientist having dealt with the "Thermodynamics of Small Systems." [9,10]. It was used shortly thereafter by Chamberlin to describe internal, local fluctuations in bulk materials for a unified picture of paramagnetic behavior of ferromagnetic materials [11]. By early May 2008, there were 36 publications making use of the concept of nanothermodynamics, in contrast to 423 papers that dealt with both thermodynamics and small phases [2]. In the present review, I want to deal with *nanophases*. This concept had been applied in 2814 publications [2], with the first publications in 1987 by Eicke [12] for research on microemulsions and in 1988 by Siegel and coworkers [13] on the synthesis of sintered titania. These initial references to research on small objects cover many different fields and come from a broad range of countries [3,5–13].

Semicrystalline, flexible macromolecules were recognized from the beginning to have small dimensions. For example, lamellar crystals of gutta percha were shown in 1938 to be only 27 nm thick (in the chain direction) [14]. This meant for our own research, which began about 50 years ago, that the phases in the samples we measured in our calorimeters were known to be very small microcrystals. The new term nanophase was used first, when my student Dr. W. Chen arrived at a need for a definition of special phases when studying in his thesis work the "Characterization of the Thermotropic Mesophases by Thermal Analysis and Solid State ^{13}C NMR" (University of Tennessee at Knoxville, TN, 1992–1996). The detailed description of nanophases for small and large molecules and what separates them from microphases was given thereafter in 1999 in an extensive review [15]. For the definition of the term nanophase, one must know the possible types of molecules [16 (vol. 3, p. 4),12] and distinguish the different possible phases [17,18] and then investigate the changes of properties with phase size [15,19]. This hierarchy of knowledge needs not only the consideration of structure, but also of large-amplitude molecular motion. The time scale of this large-amplitude motion is much further removed from human experience than the (invisible) nanophase. Large-amplitude molecular motion is encountered in translational, rotational, and conformational motion. Generally, such motion does not occur in the solid state and has time scales of the order of magnitude of picoseconds (10^{-12} s). Assuming one second in time is the equivalent to the diameter of the above-mentioned pin head, we need now to bridge a factor of 10^{12} instead of 2.5×10^4 to reach human experience [17]. After these basic facts have been clarified in the present review, brief descriptions are given for a selection of one-component nanophases produced by "top down" or "bottom up" techniques, and of multi-component nanophases.

2. Basic terms and historical links

A first, observation-based, macroscopic view of matter from antiquity to today is summarized in Fig. 1. It suggests the elements and qualities of matter as proposed by Empedokles in the 4th century BC. The modern equivalents are given in parentheses and represent the basic three phases and the link to thermodynamics by interpretation of fire as temperature, heat, and energy. The same geometrical figure as in the center is used today as logo for the ICTAC, the International Confederation for Thermal Analysis and Calorimetry [20], using the upper triangle as an indication of the science of *Thermal Analysis and Calorimetry*. Calorimetry at constant pressure (p) uses the intensive variable temperature (T), and the extensive integral function heat (H), a form of energy. The thermal analysis adds to these variables time (t) [21].

The experiment-based, microscopic view of matter was proven in 1810 [22] with the understanding of small molecules. About 100 years later, it was expanded to large molecules with the development of X-ray diffraction [23]. Fig. 2 completes the picture after the work of Staudinger, who gave flexible large molecules the name macromolecules, and proposed in his Nobel Lecture [24]: "The low molecular weight organic compounds contain up to at most 10^3 atoms . . . (and) . . . up to now, one cannot give an upper limit for the size of the macromolecules. Macromolecular compounds with a molar mass of several million are known."

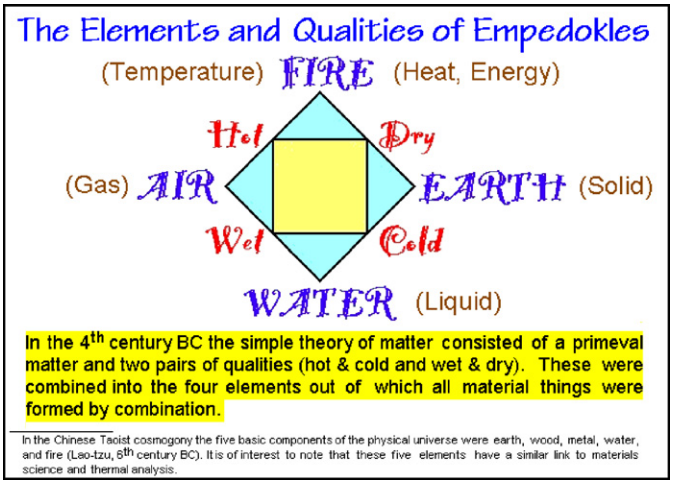

Fig. 1. The phases and thermodynamics linked back to antiquity (the modern interpretation is given in parentheses) [21].

One certainly needs to distinguish between rigid and flexible macromolecules because of the impossibility of the rigid macromolecules to melt or sublime without breaking strong bonds (metallic, ionic, or covalent). Rigid macromolecules lose their molecular integrity when leaving the solid state. Once one accepts this simple classification of all molecules, one can link each molecule type to a specific, macroscopic phase-behavior, as summarized in Fig. 2 [17,21]. This modern scheme includes all molecules and obviates the need to specify separate inorganic, organic, and biomolecules. All of these have representatives in each class and all can be made or altered in vitro. Naturally, not all small and flexible molecules reach all the indicated phases, some may thermally decompose before reaching the appropriate phase transition temperature.

The three classical phases, as given in Fig. 1, do not fully suffice to describe matter. This arises mainly because the term *solid* has

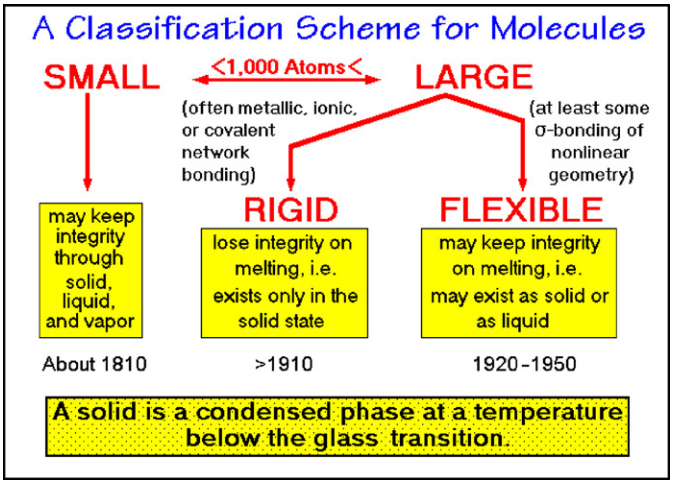

Fig. 2. Types of molecules, the years of discovery, and their phase properties [21]. The operational definition of a solid is given at the bottom.

Please cite this article in press as: B. Wunderlich, Thermodynamics and properties of nanophases, Thermochim. Acta (2008), doi:10.1016/j.tca.2008.10.026

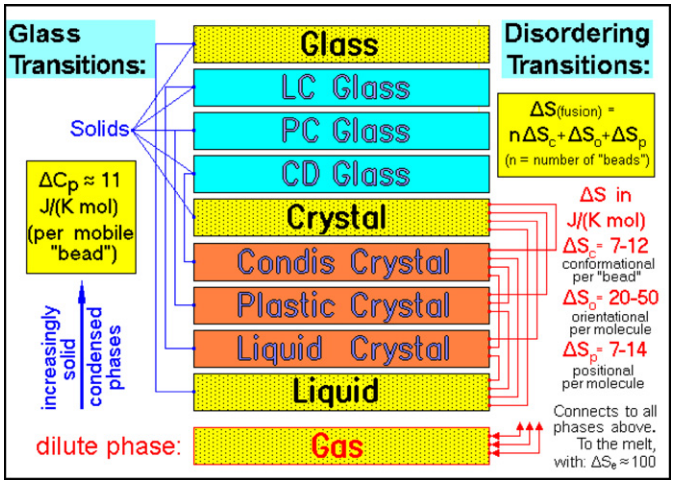

Fig. 3. The ten basic phases of matter derived from their macroscopic appearance and behavior, as well as molecular order and large-amplitude motion [21].

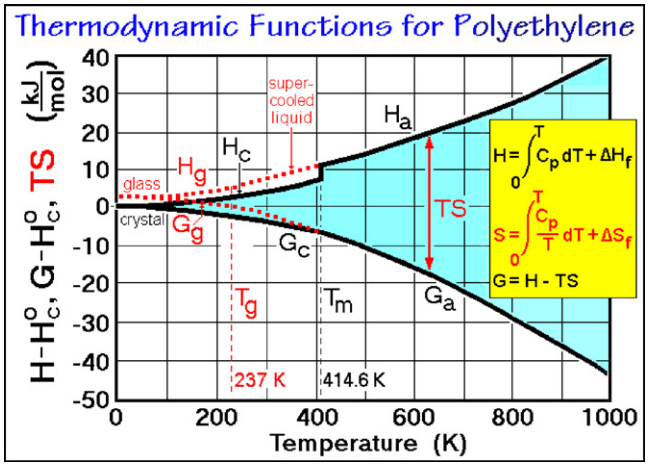

Fig. 4. The integral thermodynamic functions of polyethylene, as derived from measurements of the heat capacities and transition temperatures [21]. The subscripts a, c, g, and m refer to amorphous, crystalline, glassy, and melting. H_c° is the (unknown) enthalpy of the equilibrium crystal at 0 K. The base mole is that of the CH_2-group of molar mass 14.03 Da.

no generally accepted operational definition [25]. As a noun, it was entered in the 15th century into the English language from the Latin [4] with the meaning: "A substance that does not flow perceptibly under moderate stress, has a definite capacity for resisting forces, which tend to deform it, and under ordinary conditions retains a definite size and shape." As an adjective it was defined as neither "gaseous nor liquid." After studying many small and large molecules with respect to their thermodynamic phase transitions during the last 50 years [26], we proposed the operational definition listed at the bottom of Fig. 2 [27]. The operation answering the question 'solid or not?' is a measurement of the heat capacity, C_p, through the glass transition temperature, T_g. At low temperature, the solid C_p has the vibration-only characteristic of a solid, at high temperature, it is that of a liquid with some of the vibrational modes having changed to large-amplitude motion. Measuring mechanical properties, the same glass transition corresponds to the "brittle point" and the viscosity reaches a universal value of 10^{12} Pa s [22], satisfying the common dictionary definition of a solid [4].

With a more precise definition of a solid, it is possible to identify ten phase types, based on macroscopic appearance and behavior, as well as on molecular order and large-amplitude motion. Fig. 3 shows such a schematic [28] which includes all mesophases [29]. The term mesophase was coined to describe phases of intermediate order [30]. The five top phases are solids, i.e., they are below their respective glass transitions. The crystal, often mistakenly considered the "quintessential solid" needs some special attention in this scheme of the basic phases of matter. As can be seen on the right side of Fig. 3, the crystal is connected to all non-solid phases with a disordering transition, which increases the entropy by ΔS, depending on the type of large-amplitude motion connected to the disorder. The direct transition between crystal and melt, the melting transition, naturally, is normally also connected with a change of its C_p from that of a solid to a liquid. It, thus, is not only a disordering transition with a change in entropy, a first-order transition [31], but according to the definition given above, also a glass transition. Only the last makes it a solid-to-liquid transition. Indeed, it was found that some crystals may attain large-amplitude, liquid motion without changing their crystal structure, and then, have a T_g below the melting temperature, T_m [27].

With the basic definitions of Figs. 2 and 3, one must now look at the already mentioned changes of properties with decreasing size. The thermodynamic description of the *macrophase* was developed at the end of the 19th century [32]: The phases consist of homogeneous, macroscopic volumes of matter, separated by well-defined surfaces of negligible influence on their thermodynamic functions. These functions are based on the measurement of C_p starting at 0 K and the evaluation of the integral quantities enthalpy, H, entropy, S, and free enthalpy, G. Fig. 4 shows an example of such a description for the liquid, crystalline, and glassy phases of polyethylene, based on the tables of the ATHAS Data Bank [33].

As the mass of matter becomes smaller, the surface effect has to be considered [32]. This effect becomes dominant in *microphases*, phases with at least one dimension less than one micrometer. Since the surface free energy describing this effect is always positive, a given mass will try to minimize the surface area, and, if additional sample mass is available, smaller particles are metastable relative to larger ones. To describe the free energy of a microphase, one can use the Gibbs–Thomson equation [10,34,35]. To calculate the lowering of the melting temperature, ΔT_m, for a small volume, V, it takes the format:

$$\Delta T_m = \frac{\sigma T_m^\circ A}{\Delta h_f \rho V} \quad (1)$$

where σ is the specific surface free energy; T_m°, the bulk equilibrium melting temperature; A the surface area; Δh_f, the specific heat of fusion (per gram); ρ, the density of the crystal; and V, the volume. For a 10 nm thick lamella of polyethylene, for example, ΔT_m is 26 K when one considers that only the fold surfaces contribute to σ [16 (vol. 3, p. 32)].

The glass transition, in contrast to the melting transition, is little affected when going from macrophase to microphase. It has its origin in local domains within the phase and occurs over a range of temperature depending on the distribution of the neighborhood energetics. In one-component phases, the glass transition range is commonly 5–10 K when measured by a tangent through T_g [21 (p. 764)]. An early description of the glass transition in terms of these local domains was the hole theory. The holes were given the excess energetics of the surrounding matter. For polystyrene, for example, the hole was computed to be about 0.3 nm in diameter [36]. Surrounding the hole by one or two molecular layers of matter to carry out the large-amplitude motion, the domain has an overall dimension of the order of magnitude of 1–2 nm and the (time-dependent) breadth of the transition is explained by a distribution of holes of different instantaneous structures.

What then are nanophases, are they not just small microphases? Considering the condition that a phase must be homogeneous, one can set the lower limit of all phases at a diameter of, perhaps, 0.5 nm. A volume of this diameter may contain 10–50 atoms,

Please cite this article in press as: B. Wunderlich, Thermodynamics and properties of nanophases, Thermochim. Acta (2008), doi:10.1016/j.tca.2008.10.026

too few to be called homogeneous. A separate nanophase would have a justification only if phases with sizes larger than this limit would already have lost all their interior bulk phase and show interactions between opposing surfaces, such that, for example the Gibbs–Thomson equation does not hold anymore, and that T_g is moved from its bulk value. This new phase would then be a nanophase with different thermodynamic properties from the microphase. Its range of dimensions is expected to be somewhere between 0.5 and 50 nm, different for every material.

A complication for such small phases would be that linear macromolecules can easily be much longer than the nanophase, and the molar volume for the higher molar masses may even exceed the nanophase size. An extended-chain molecule of polyethylene of 10,000,000 Da molar mass, for example, would have a length of 91,000 nm and a diameter of about 0.5 nm. It can easily cross the phase boundaries of many adjacent nanophases, and a droplet of such molecule would have a diameter of about 26 nm and may have microphase properties.

To summarize this discussion of the phase sizes, *macrophases* should be describable without need to consider their surface effects (except for justifying their geometric shapes which are set during phase formation by minimizing the surface free energy [37]). *Microphases* occur on reducing the size below one micrometer and the surface free energy affect their properties. *Nanophases*, finally, are to be found in the size range of 0.5–50 nm, but are different from microphases only, if there is no bulk phase enclosed by the surfaces (this means that the upper limit of nanophases will vary with composition and property of the phase boundaries). The lower limit of thermodynamic descriptions is expected to be reached below 0.5 nm.

From this set of definitions, it becomes clear, that frequently carelessly declared nanophases often are actually long-known microphases and not worth the attention they are getting. Only if it can be proven by evaluation of the phase properties that there have been changes from the microphase, should the term nanophase be applied.

3. One component nanophases

3.1. Nanocrystals produced by building atom by atom or molecule by molecule

Sequential deposition of atoms, small cluster of atoms, or even macromolecules from the gas phase or from reactions in solutions of precursors are examples of the "from the bottom up" techniques of nanophase construction. Colloidal gold (nanogold) was made already by the ancient Romans to color glass, and gold sols were a part of the alchemists' reagents. Today, monodisperse gold sols in water or organic solvents are made down to 2 nm particle size by reduction of $HAuCl_4$ in the presence of proper surfactants. In 1847, it was suggested by Faraday [38] that the different colors of these gold sols were due to the smallness of the particles.

The breadth of the field of nanophase science can be illustrated by many long-known observations, now known to be caused by the changed properties of nanophases. The optical appearance of finely divided deposits on a substrate usually are black, irrespective of the bulk color (as in the case of the metal blacks and carbon blacks). There is often a largely increased chemical and catalytic reactivity in specially deposited elements (seen in the long-recognized pyrophoric Fe and Pt-black) [39]. Under proper conditions, ordered structures may develop which are uniquely different from the bulk phases (examples are crystals growing from vapor deposits of Ar, the fullerenes contained in carbon black, and the production of nanodiamonds instead of graphite which is the thermodynamically stable polymorph in macrophases). Quantum dots with properties between bulk phases and discrete molecules are known (from

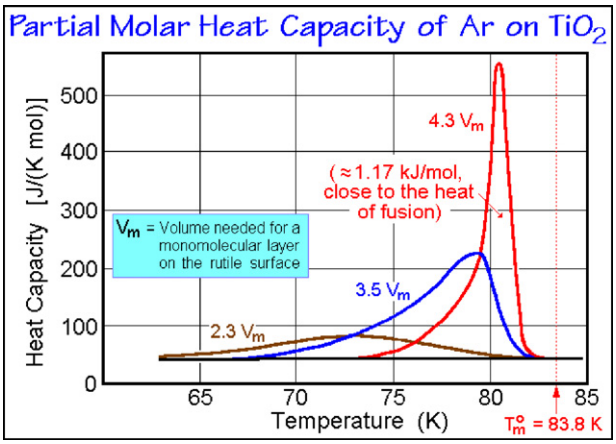

Fig. 5. Partial molar heat capacities of adsorbed Ar. Measured at temperature increments as small as 0.3 K in the region of largest latent heat absorption. The boiling point at STP is at 87.3 K. The thickness was estimated in multiples of the monomolecular thickness measured by the BET method (≈1.35 g on 39 g of rutile) [40].

nanophases of semiconductors like CdSe and PbSe). Finally, composites with finely divided particles may increase tensile strength and abrasion resistance (as seen for carbon black in rubber).

Fig. 5 illustrates early observations of the change in thermal properties with the amount of deposit in the case of gaseous Ar absorbed on TiO_2 (rutile) [40] and measured by low-temperature adiabatic calorimetry [41]. At an average adsorption thickness of 1.6 times the monomolecular volume, V_m, no latent heat was observed, and above $V_m = 5$, the crystals seem to approach the behavior of a microphase. In between, nanocrystals with quite different properties can be assumed to account for the broad and strongly lowered melting range, as well as the decreasing heat of fusion. The fact that the melting temperature is lowered, is an indication that there is no major attraction across the rutile/argon interface which otherwise would increase T_m.

A strong interaction was proven for the adsorption of paraffins on graphite by high-temperature atomic force microscopy, AFM. Fig. 6 illustrates the experiments [42]. The paraffin, $C_{390}H_{782}$ of an extended-chain length of about 49.7 nm, was crystallized from xylene solution into lamellae which had their chains 5-times folded to yield a ca. 10 nm crystal thickness. The crystals could be spin-coated wet, as a single-layer onto single-crystalline graphite with the axis of the molecular chain normal to the (0 0 1)-surface of the graphite. The annealing through unfolding of the chains was followed by melting at about 400 K. This melting is accompanied by spreading of the alkane onto the substrate, leading to the crystallization of epitaxial monolayers. This nanofilm is composed of ribbons with the alkane chains lying parallel to the substrate. The chain tilt detected in these ribbons vanishes during a structural transition occurring prior to the complete melting, about 55 K *above* the melting point of the bulk material. The polymorphism and increased melting temperature of the paraffin documents that the behavior of the nanophase is different from that of the bulk paraffins. This higher melting temperature of the epitaxial paraffin probably supplies also the reason for the practically reversible crystallization and melting of paraffins without the need of primary nucleation, as documented by temperature-modulated differential scanning calorimetry, TMDSC (up to a critical length of about 10 nm) [43]. The adsorbed, ordered paraffins on appropriate surfaces, such as the surface of the aluminum sample pans in a calorimeter or the glass capillary in a melting-point apparatus seem to serve as primary nuclei.

Having recognized the importance of the surface substrate on interface-supported nanophases, Fig. 7 illustrates the change of the properties of spherical gold nanoparticles with time and tem-

Please cite this article in press as: B. Wunderlich, Thermodynamics and properties of nanophases, Thermochim. Acta (2008), doi:10.1016/j.tca.2008.10.026

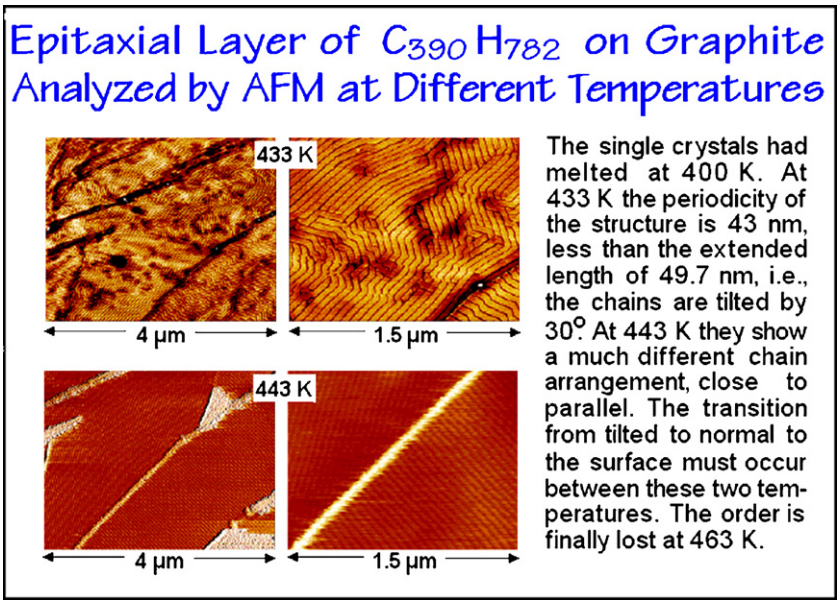

Fig. 6. Polymorphism and increase in melting temperature observed on a nanophase of $C_{390}H_{782}$, epitaxially crystallized on the (0 0 1) surface of graphite [42].

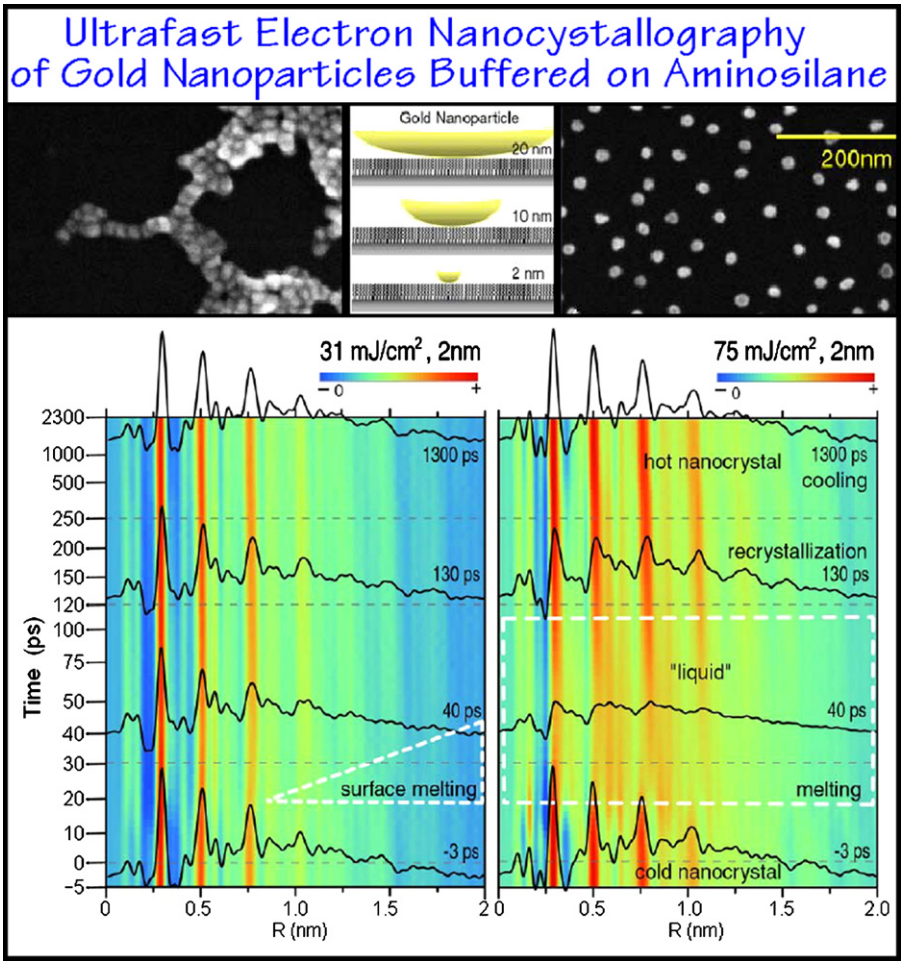

Fig. 7. Observation of melting and recrystallization of 2 nm gold nanophases for two different energy additions as function of time, based on femtosecond laser experiments [44]. Top left and right are scanning electron micrographs of the 20 nm particles with and without AEAPTMS. A schematic of the particles buffered from the Si substrate is given in the top center. The bottom displays are the radial electron distribution functions as a function of time, overlaid with curves at selected times for incomplete (left) and complete melting (right). The curve at −3 ps is the pre-pulse reference curve. The melting effect is marked by the thick dashed lines.

Please cite this article in press as: B. Wunderlich, Thermodynamics and properties of nanophases, Thermochim. Acta (2008), doi:10.1016/j.tca.2008.10.026

perature [44]. The nanoparticles were deposited from a colloidal solution and separated from the Si(1 1 1) surface of the substrate by buffering with a self-assembled, monomolecular layer of [3-(2-aminoethylamino)propyl]trimethoxysilane, AEAPTMS, as shown at the top right. The layered structure is illustrated to scale in the top-center schematic. Without the buffer, the Au nanoparticles cluster, as seen in the top-left picture, and would not act independently. Next, photo-induced melting and subsequent recrystallization was analyzed with an 800 nm wavelength, femtosecond (1 fs = 10^{-15} s) laser for different diameter Au-nanophases. The same laser was also used to produce 40 fs electron pulses via a photo cathode for ultrafast electron crystallography. The analysis of the 2 nm particles is shown at the bottom of Fig. 7. The left results are from a low energy pulse, the right results, from a high-energy pulse. Separate experiments put the equilibrium melting temperature of Au at 1338 K, a 20 nm diameter microphase at ca. 1300 K, that of a 2 nm diameter microphase at ca. 800 K [45]. Values which exceed Eq. (1) for a microphase (which would predict only a ten-fold change in melting-temperature lowering on going from 20 to 2 nm). As expected, the crystal structures of the nanophases deviates from the FCC structure of the bulk, supplying a reason for the increased melting-temperature lowering with size.

In Fig. 7, the 31 mJ cm^{-2} photopulse on the nanophase expands the volume with little adjustment of the bond density below 1 nm, an effect interpreted as surface melting. At 75 mJ cm^{-2}, in contrast, the bond densities are changed throughout. The nanophase melts within 18 ps and is recrystallized at 110 ps, as indicated. This photo-melting mechanism is distinctly different from the recrystallization which is similar to a reverse thermal melting. Both processes have been analyzed relative to the phonon dynamics [44].

A general thermodynamic method to understand metastable phase formation at the nanoscale was proposed by Wang and Yang in a review with 321 references [46]. This nanothermodynamics is different from the approach by Hill [8–10] and emphasizes a size-dependent surface free energy which forces the nuclei into a different structure. Supporting examples are the nucleation of diamond instead of graphite on growth of nanophases during chemical vapor-phase deposition and, similarly, of cubic BN instead of hexagonal BN. This approach might also improve the classical nucleation theory of crystal growth. Further experiments and molecular dynamic calculations are summarized next, testing the limits of setting up a nanothermodynamics.

Nanophases are composed of sufficiently small numbers of atoms so that their behavior can be simulated by molecular dynamics calculations. The first set of simulations chosen to get insight into paraffin and polyethylene nanocrystals was based on unrestrained assemblies of paraffin chains of 50 or 100 carbon atoms in length in a constant pressure simulation [47]. First, one can check the skeletal vibrations and the introduction of conformational defects. Fig. 8 illustrated the changes of the bottom portion of the center chain in a crystal in steps of 0.1 ps at 320 K. The details of the skeletal vibrations and the mechanism of the formation of a conformational defect (2 g1 kink defect) and their time scales are obvious. The phonon velocity along the chain direction agrees with the measured speed of sound. The length of the chain affected by the specific large-amplitude motion which produces the defect is 1–2 nm. The time scale of the three-phonon collision is 0.5 ps, and the life-time of a large number of defects analyzed similarly at the same temperature, is 1–3 ps.

Next, one can check the concentration of the conformational defects as a function of temperature by simulation at decreasing temperatures. The data are presented in Fig. 9 for a nanophase of 192 $C_{50}H_{100}$ chain segments [48]. The simulations agree well with the experimental IR data of gauche conformations in paraffins [49] and fit the increase in C_p in crystalline polyethylene beyond that of the vibrational motion [21].

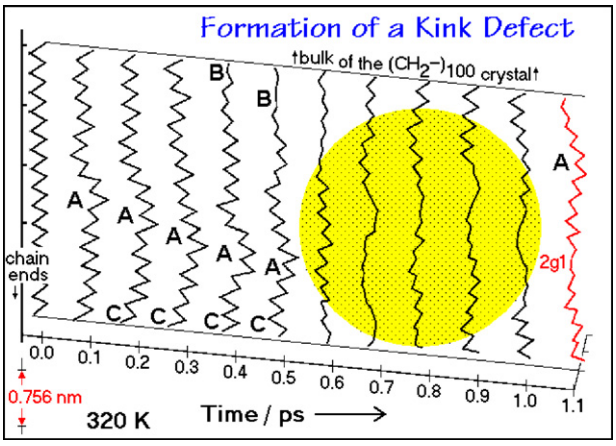

Fig. 8. Motion of the end of a single chain in the center of a nanocrystal of $C_{100}H_{200}$ drawn as a function of time. Addition of kinetic energy at time 0, observation of translational (A), torsional (B), and longitudinal (C) vibrations and the formation of a conformational defect (between 0.5 and 1.0 ps). The life of the defect created was 2.1 ps [47].

The time to reach thermal and mechanical steady state after instantaneously raising the vibrational energy to a given temperature could also be calculated. For this calculation, the average kinetic energy of a nanocrystal was followed for 100 ps as shown in Fig. 10. The kinetic energy reaches steady state within 10–20 ps, followed by slow cooling (due to rounding errors in the simulation). The temperature fluctuations shown in Fig. 10 reach ±5 K [50].

Finally, the structures of the simulated nanophases of $C_{50}H_{102}$ at steady state are displayed in Fig. 11 [47]. The five top figures illustrate a view along the crystallographic *c*-axis (chain axis) at different temperatures, and the two bottom drawings show the two lateral views at 234 K. The melting temperature of the bulk phase is 365 K, but considerable disorder exists below T_m°. Also, there is a distinct difference in the packing density and order when going from the interior of the crystal to its surface. The bulk monoclinic order is not retained in any of the nanocrystals. The same is true when starting with the stable orthorhombic crystal structure, both approach a hexagonal packing as seen in the "rotor phases" of the paraffins.

At the time of this work, interpreting these shifts in crystal structure could not be explained definitively. Three reasons were considered [47]: (1) The shift may have been a flaw in the simulation because the calculations made use of a united-atom model

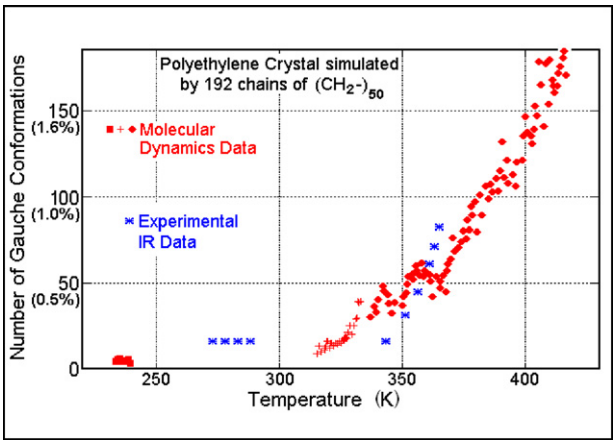

Fig. 9. Comparison of the change of conformational defects as a function of time, evaluated by molecular dynamics simulation and experimental data by IR spectroscopy [48].

Please cite this article in press as: B. Wunderlich, Thermodynamics and properties of nanophases, Thermochim. Acta (2008), doi:10.1016/j.tca.2008.10.026

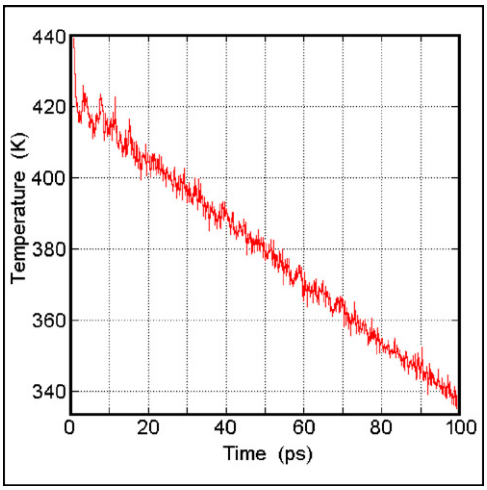

Fig. 10. Fluctuations of temperature on a picosecond scale when cooling a nanophase of 192 $(CH_2)_{50}$ chains, simulated by molecular dynamics calculation [50].

(i.e., each CH_2-group was represented by a single united-atom of equivalent mass and shape, allowing simulation of larger crystals over longer periods of time). (2) The small size of the modeled crystal. (3) The limited weak force field used for the computation of the long-range, non-bonded interaction, truncated at 1.0 nm for each atom (also for economy in computing-time).

Additional work to decide on the main reason for the change in crystal structure included enclosing the simulated chains in a rigid shell of orthorhombic chains (leading to a constant volume simulation). In this case, the orthorhombic structure, with the usual defects, was retained, suggesting, larger crystals would favor the stable, orthorhombic crystal. Placing a mobile layer next to a fixed orthorhombic surface also kept this symmetry, but only for a limited number of layers. A few simulations were also carried out with explicit H-atoms for the same size nanocrystals as shown in Fig. 11, now with 28,800 atoms instead of the prior used 9600 [51]. The initial, stable orthorhombic structure also changed to a packing not far from hexagonal, but not the full "rotator" phase seen in Fig. 11. The uncertainty due to the chosen non-bonded force field became even larger in this case of the explicit hydrogen simulations because the non-spherical shape of the force field of hydrogen [52]. These results could not quite exclude the reasons other than crystal size as the cause of change in crystal structure. By now, however, the

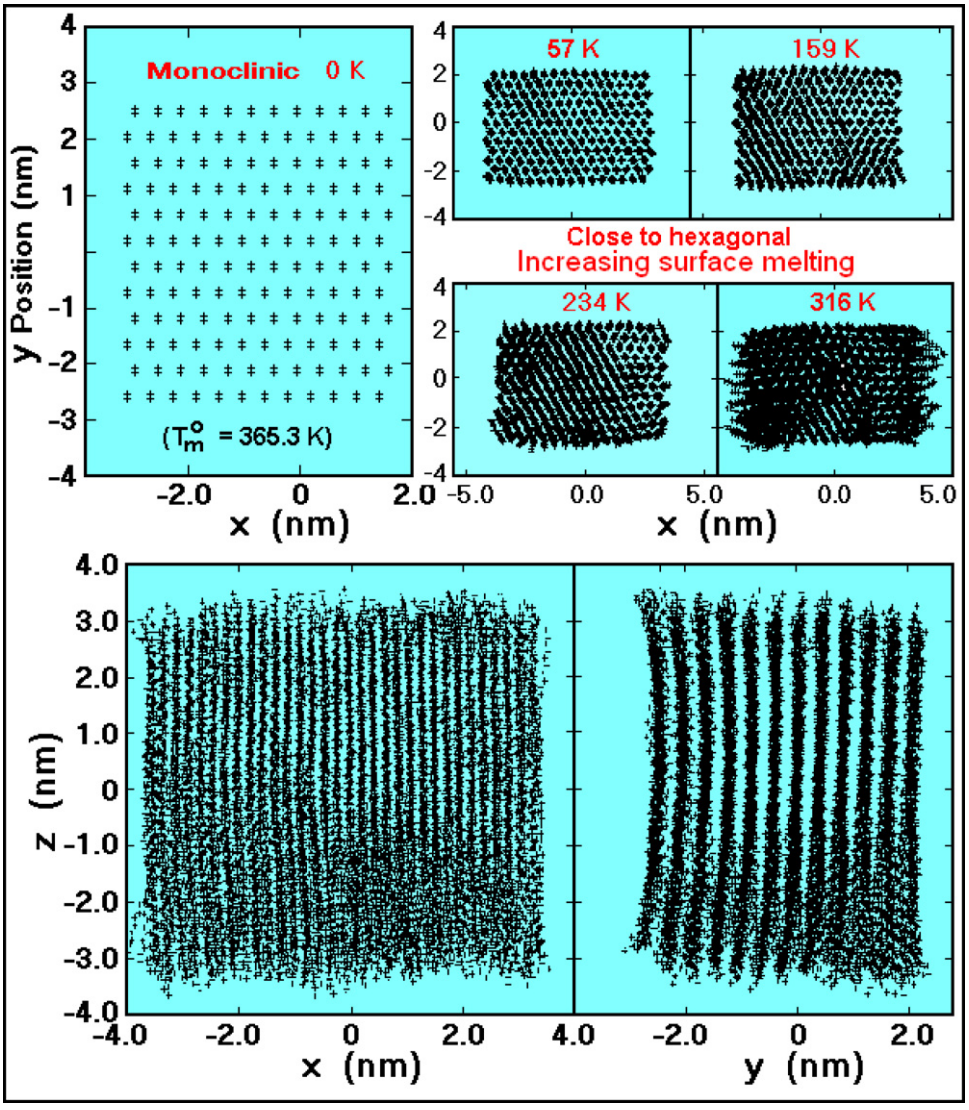

Fig. 11. Molecular dynamics simulation of a paraffin nanocrystal [47]. Right upper pictures are projections of 192 $C_{50}H_{100}$ chains at the given temperature after equilibrium was attained. The left upper picture is an enlarged section of the initial structure at 0 K. The two bottom pictures are projections at right angles to the chain direction at 234 K.

Please cite this article in press as: B. Wunderlich, Thermodynamics and properties of nanophases, Thermochim. Acta (2008), doi:10.1016/j.tca.2008.10.026

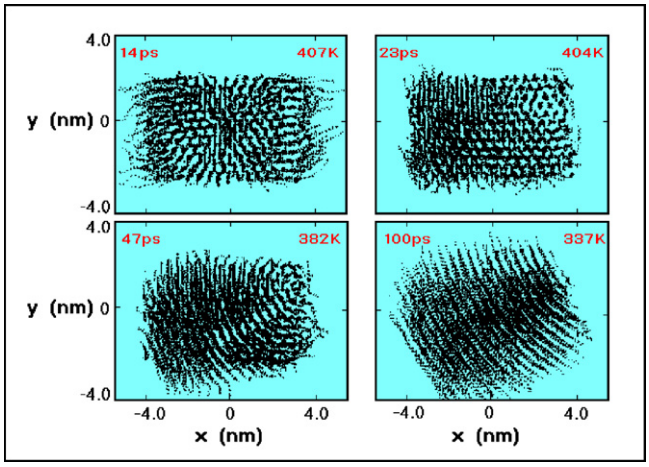

Fig. 12. Change of the structure of a nanocrystal of Fig. 11 heated above the melting temperature, followed by cooling [53]. (Compare to the time scale of Au nanocrystals heated above the melting temperature, followed by cooling, shown in Fig. 7.)

greater stability of a hexagonal-like phase in nanocrystals seems more likely, and a new series of simulations as a function of size would be of interest. Such change in crystal structure with smaller crystal size is also supported by the commonly observed condis-crystalline packing of paraffinic segments attached as side chains or phase-separating within polymer chains [15].

Fig. 11 also documents that the interior of the simulated nanocrystals is not uniform in density and structure. One sees regions of different packing and orientation. From the side-view, one notes a continuous variation of density and disorder towards the surfaces. The surfaces with chain ends become increasingly rough as the melting temperature is approached.

A simulation of melting and recrystallization, as seen for the Au nanocrystals in Fig. 7, is reproduced in Fig. 12 for $C_{50}H_{102}$, and illustrated with Fig. 12 [53]. The time scale of the disordering and reordering is similar to the Au nanocrystal, but the melting on heating above T_m° is not complete, as it is in Fig. 7. The internal flexible chains are kept largely parallel. The time scale for collapse of an isolated chain to a random coil was estimated by molecular dynamics simulation to be ≈30 ps and can only proceed consecutively from the surface to the interior, as suggested in Figs. 11 and 12 [47]. Vibrational and isolated large-amplitude motion equilibrate in times of ps, while cooperative processes, such as the collapse of flexible chains, may take much longer. The simulation of melting and recrystallization, thus, were different from the slow thermal processes which occur with continuing equilibration of all types of molecular motion.

Similar to the above-mentioned Au, C, BN, and paraffins, the synthesis of nanocrystalline metal oxides results often in crystals which are structurally different from the bulk material [54]. An example is Al_2O_3 which has been studied, besides by structure analysis and molecular dynamics simulations, also by identifying the surface properties with water adsorption experiments, including microcalorimetry, thermogravimetry, and high-temperature solution calorimetry [55]. The stable bulk phase is corundum, α-Al_2O_3 of hexagonal crystal structure. The stable nanophase is γ-Al_2O_3 of cubic crystal structure and has a lesser density and higher entropy. Measurements and molecular dynamics calculations of surface and bulk energies showed that the higher G of the γ-Al_2O_3 at negligible specific surface area can be overcompensated by its lower surface free energy which becomes the dominating term above 125 $m^2\,g^{-1}$.

Finally, analyses of TiO_2 and ZnS are mentioned for their differences in phase transformation mechanisms between nanophases (anatase and wurtzite structure, respectively) and the corresponding bulk phases (rutile and sphalerite structure, respectively) [56]. Results from thermodynamic analysis, kinetic modeling, and molecular dynamics simulations were used in the discussion. The structures were characterized by transmission electron microscopy, X-ray diffraction, synchrotron X-ray absorption and scattering, and UV–visible spectroscopy. Similar results as for the example of Al_2O_3, above, were found as a function of particle diameters with crossovers in phase stability. For the growth and phase transition, oriented attachment of nanoparticle to nanoparticle was suggested to allow a kinetics not observed in macroscopic materials, where Ostwald ripening via transport of isolated atoms or molecules is expected. The changes in the mechanism were deduced from the difference in growth kinetics.

These examples of one-component nanophases produced by building atom by atom or molecule by molecule suggest that the stability depends on the details of both, surface *and* interior structure [56]. The excess energy need not be confined to the surface, as assumed in [55], a conclusion, also reached based from the simulation in Figs. 11 and 12 [47]. In addition, one should remark that the interior volume is sufficiently small, so that its structure varies considerably within this volume. Any mean-field calculations, then, can only be a first approximation for a nanophase thermodynamics, just as a simple surface free energy change with size may be insufficient for the description of the stability of a nanocrystal.

3.2. Nanocrystals produced by reducing the size of macrophases or microphases

Reducing the size of macrophases with miniaturized manufacturing was already discussed by Feynman [1]. This sequence, however, of making increasingly smaller and smaller machines, seems to be limited and one has to turn to special techniques. One cannot yet make metallic nanophases on a miniaturized lathe or cut nanodiamonds from big crystals with the traditional means. More successful methods are the production of nanodroplets by electrospraying [57] or the shaping of nanofibers by electrospinning [58,59] and the extreme expansion of ductile films into nanofoils. (Since antiquity one has made ≈100 nm thin gold leaf, and more recently, nanoporous Au and Pt with largely different properties was made [60].) Photolithograpy can be increased in resolution by using electron or ion beam lithography and then allowing large-volume printing of nanophase patterns. A multitude of etching techniques can reduce larger phases ultimately to nanophases. Finally, solutions can be made sufficiently dilute so that macroscopic droplets or films may leave nanophase particles if the solvent can be removed by evaporation or replaced by a non-solvent for the solute [61,62]. Next, the results of some of these methods to make nanophases will be described when applied to macromolecules. It will be shown that a unique analysis method is available when studying glassy nanophases as they are frequent in polymers.

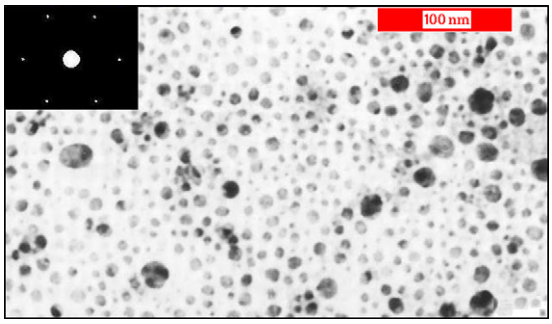

Fig. 13. Single-molecule, single-crystals of poly(oxyethylene) grown from solution [61]. The electron diffraction pattern in the corner proves single-crystalline character.

Please cite this article in press as: B. Wunderlich, Thermodynamics and properties of nanophases, Thermochim. Acta (2008), doi:10.1016/j.tca.2008.10.026

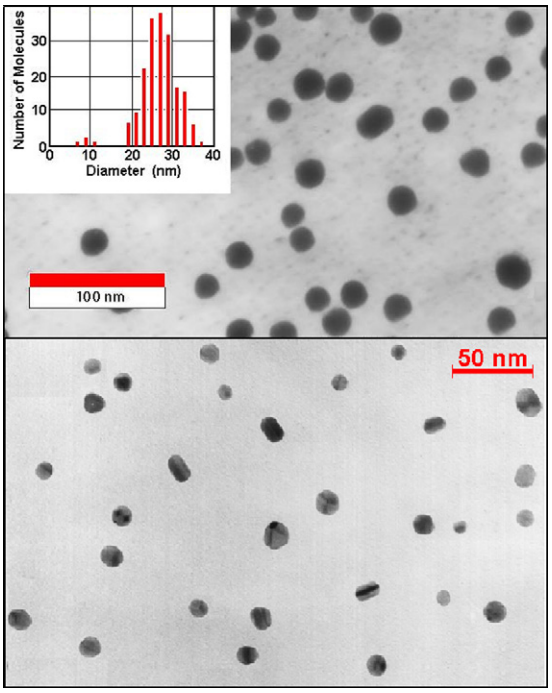

Fig. 14. Single-molecule particles of polystyrene. Top figure, atactic, amorphous, glassy spheres [61]. Bottom figure, isotactic single-molecule single-crystals [62].

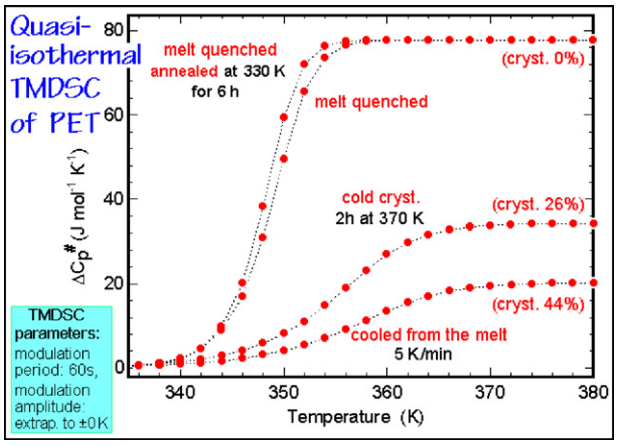

Fig. 15. The change of heat capacity of various poly(ethylene terephthalate)s in the glass transition region, measured by TMDSC [63].

Fig. 13 illustrates the collection and analysis of single molecules of poly(oxyethylene), POE, crystals [61]. A broad distribution of number average molar mass of 6.7×10^5 Da was dissolved in benzene to 2×10^{-4} wt.%, a concentration below the critical overlap concentration of the expanded random coils of the macromolecules. The benzene solution was then spread drop by drop on a water-filled Langmuir balance at 353 K. The benzene was evaporated and the POE precipitated (hot water is a non-solvent for both benzene and POE). The POE molecules crystallized, and were concentrated by compression with the balance and then transferred to an electron microscope grid. The electron diffraction pattern proves a single-crystalline structure close to that of bulk-grown, lamellar crystals. The lateral size-distribution of the lamellar crystals matches the molar mass distribution. The crystals assumed the folded-chain morphology of ≈20 nm thickness, measured by their shadow length, and known from bulk-grown lamellae. This fold-length is much less than required for equilibrium of the limited amount of POE per crystal.

The top electron micrograph of Fig. 14 illustrates similarly prepared droplets of a fraction of amorphous, atactic polystyrene, PS, of 1.3×10^6 Da. The molar mass distribution calculated from 200 particles shown in the corner of the figure matched the distribution measured by size-exclusion chromatography, including the small fraction of low molar mass impurities. Later, such amorphous PS single (and multiple) molecules could be produced by electrospraying [57]. Using isotactic PS of molar mass 1.5×10^6 Da in a similar experiment as shown in the top electron micrograph of Fig. 14, the amorphous nanoparticles could be crystallized at 448.2 K by heating on the carbon support of the electron microscope grids. The bottom Fig. 14 illustrates the obtained lamellar, 14 nm thick single-molecule single-crystals [62]. Their morphology, fold length, and crystal structure (from microbeam electron diffraction) matched the results known from crystallization from the bulk [16]. Both, PEO and PS single-molecule single-crystals, thus, did not deviate observably from the crystals grown from the bulk. The lamellar bulk polymer crystals are commonly identified as microcrystals, with their melting behavior describable with the Gibbs–Thomson equation [16 (vol. 3)]. In order to reach a truly nanophase character, the lateral dimensions of the single-molecule single-crystals would have to be reduced, i.e., lower molar masses could lead to nanocrystals.

On going from the single-molecule single-crystals to semicrystalline macromolecules, one must account also for the non-crystalline fraction which is intimately connected to the crystals by tie molecules [16]. While the crystals can be characterized thermodynamically by their melting behavior via the melting-temperature lowering from equilibrium, as given by Eq. (1), and the crystallinity, as calculated from the heat of fusion decrement, the analysis of the amorphous fraction has often been neglected. Its property can be assessed in great detail by a study of the glass transition, as outlined in Section 2, above.

Fig. 15 illustrates part of a detailed study of the glass transition of amorphous and semicrystalline poly(ethylene terephthalate), PET, as a function of crystallization and annealing conditions [63]. The glass transition range of the amorphous macrophases is rather narrow when measured by TMDSC as suggested in Section 2 (top two curves, ≈8 K). Annealing a rapidly cooled glass sharpens the transition somewhat, but introduction of crystalline microphases causes a major change in the surrounding amorphous fractions. The glass transition range for the 44% crystalline sample (as measured from the heat of fusion), for example, is ≈18 K with little or no change in the temperature of the beginning of the transition. Using the above mentioned "hole theory" for a simple estimate of the kinetics of the glass transition over the transition temperature range [36,63], the activation energy for the time-dependence of the relaxation time, τ, of the holes changes from ca. 375 kJ mol^{-1} for the amorphous sample to 160 kJ mol^{-1} for the 44% crystalline sample. To keep the beginning of the glass transition the same, the logarithm of the pre-exponential factor, B, changes linearly with activation energy, E_a ($\tau = B \times e^{E_a/RT}$) [63]. Besides this broadening of the glass transition, indicative of a changing distribution of large-amplitude motion within local domains, Fig. 15 shows that the measured change in heat capacity, $\Delta C_p^{\#}$, does not scale with the amorphous fraction. A considerable fraction of the amorphous PET does not contribute to the glass transition in the given temperature region. This fraction was called rigid amorphous, RAF [64]. Its glass transition is moved to a higher temperature and may even be moved to the melting temperature, and sometimes even above the T_m [65]. Due to this change in property, expressed by the glass transition, one must call the RAF a new nanophase, leading to a three-phase picture of semicrystalline polymers which has found more general acceptance recently. The most common sizes of these three phases are in the microphase region for the crystals and the nanophase region

Please cite this article in press as: B. Wunderlich, Thermodynamics and properties of nanophases, Thermochim. Acta (2008), doi:10.1016/j.tca.2008.10.026

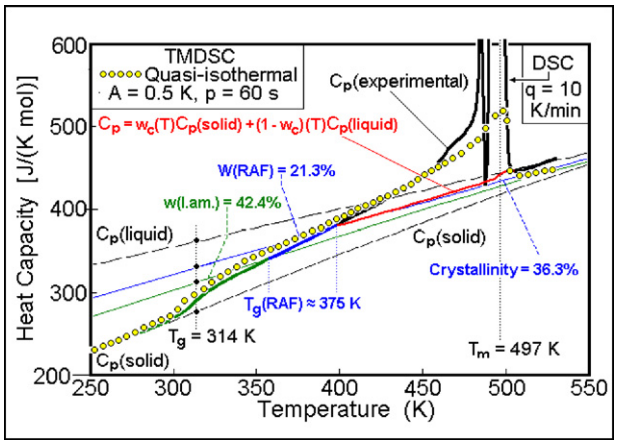

Fig. 16. The change of heat capacity of poly(butylene terephthalate), analyzed by DSC and TMDSC to identify the three phases via their glass transitions and the melting/crystallization peak [67].

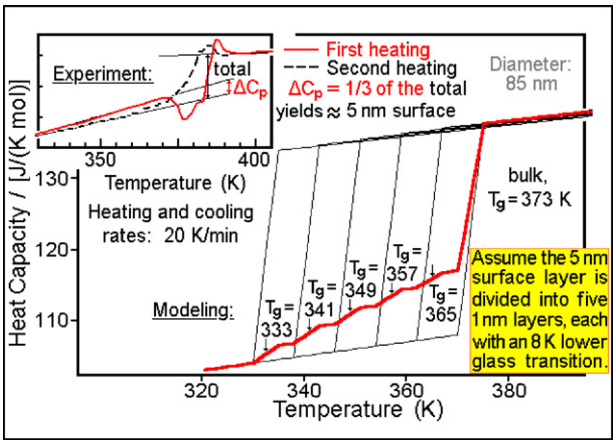

Fig. 17. Broadening of the glass transition of polystyrene microspheres of 85 nm diameter. *Insert*: Experimental data [68]. *Main plot*: Interpretation assuming a 5 nm surface layer [69].

for the mobile and rigid amorphous fractions. Electron microscopy was able to identify the three phases by the different amount of RuO_4 uptake in staining experiments [66].

Fig. 16 illustrates the detailed thermodynamic analysis of poly(butylene terephthalate), PBT, with standard DSC and TMDSC [67]. A low-temperature glass transition of the semicrystalline PBT at ≈314 K accounts for only 42.4% of the expected 63.7% amorphous fraction calculated from the crystallinity. The second glass transition is assigned to the RAF at ≈375 K and has a breadth of about 40 K and accounts for the missing 21.3%. For a full characterization of semicrystalline PBT in Fig. 16 one needs, thus, the phase description of the 36.3% crystals, to be read from the melting and superimposed cold-crystallization peak and the small fraction of reversible melting [65], the 42.4% mobile-amorphous fraction, characterized by the broadened glass transition at 314 K, and the 21.3% RAF, with its higher, also broad, glass transition at ≈375 K. Although a number of semicrystalline polymers have been analyzed in such detail [65], most have still only been qualitatively studied.

While the introduction of crystalline interfaces always moves the glass transition to higher temperature, the introduction of a free surface was shown to broaden the glass transition to lower temperature. Fig. 17 illustrates that spheres of polystyrene microphases with a 85 nm diameter show a broadening of a fraction of the glass transition to lower temperature when measured by DSC (solid curve in the insert) [68]. The glass transition is interrupted before completion by an exotherm caused by the fusion of the spheres to a macrophase. The end of the glass transition range is marked by the common, small hysteresis endotherm. The interpretation of the data suggests that the surface can be approximated by five shells, each of one nanometer thickness and an 8 K lower T_g on approaching the interface, as indicated in the main plot [69]. The conclusion from Fig. 17 is that the analyzed spheres have an overall

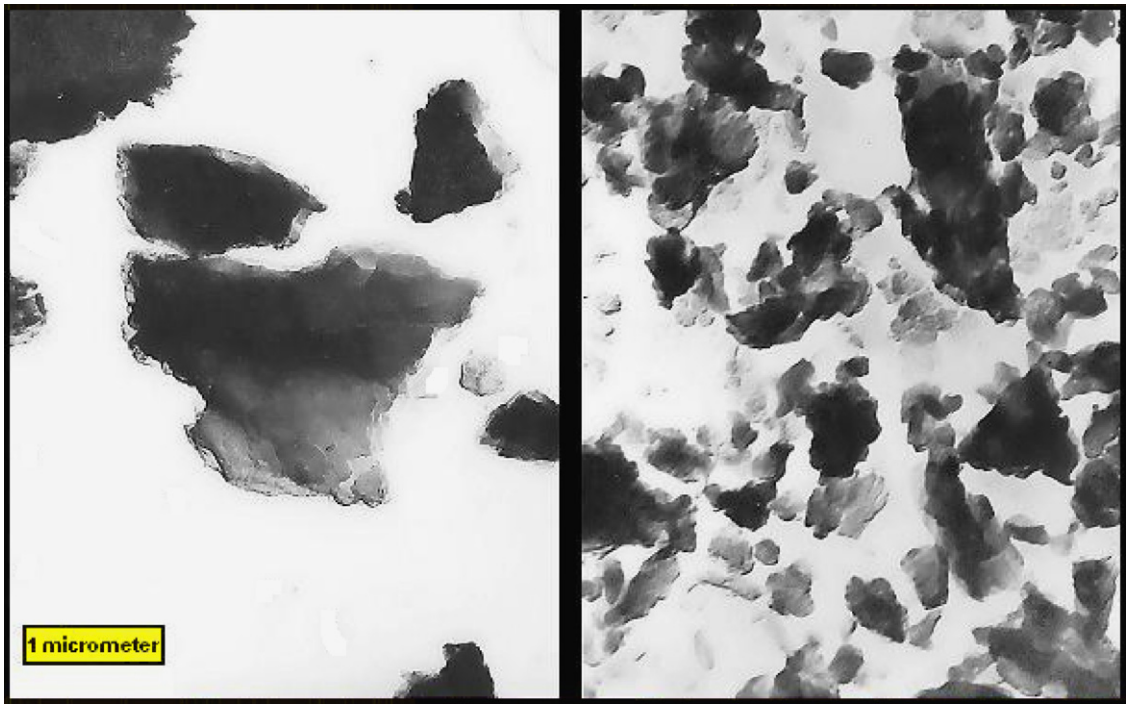

Fig. 18. Poly(ethylene terephthalate) crystals removed from semicrystalline samples by etching of the amorphous fraction with superheated water [70]. Left: A sample crystallized at 523 K after quick cooling from the melt, hydrolyzed at 453 K. Right: A sample crystallized at 413 K after quick cooling from the melt, hydrolyzed at 403 K.

Please cite this article in press as: B. Wunderlich, Thermodynamics and properties of nanophases, Thermochim. Acta (2008), doi:10.1016/j.tca.2008.10.026

5 nm surface layer of increasing T_g from the surface, at 333 K to the inner bulk of 373 K. This leads to the assumption that a sphere of 10 nm diameter would not contain any bulk phase anymore, i.e., by the above definition, it would be a nanophase.

To separate the tie-molecule interlaced phases in semicrystalline polymers, various etching methods have been developed [16]. Fig. 18 illustrates the etching of two PET samples of different crystal size to remove the amorphous phases [70]. The etching removed also the folds, so that the sample is oligomeric after treatment. The shown samples are still of microphase size, but it should be possible to etch even faster grown crystals or extend the etching time to reach the nanophase range and produce sufficiently large samples to conduct analyses with classical calorimetry. Battista [71] published electron micrographs of etched cellulose single crystals of 20–40 nm diameter and up to 500 nm lengths from native cotton fibers which are in the microphase range, as well as similarly etched crystals from fringed-micelle crystals from rayon, which were in the nanophase range with equal dimensions in all directions of 5–20 nm. Similarly, electrospun nylon 4.6 fibers of close to one nanometer diameter have been reported (6–7 nylon molecules in cross-section) [59].

The one-component nanophases produced by reducing the size of macrophases or microphases has not been analyzed as frequently. For macromolecules etching is of major importance since it not only can produce nanophase crystals, but it also allows to isolate crystals from the strongly bonded aggregate structure of semicrystalline polymers. In this way, it should be possible combining the analyses displayed in Figs. 13–17 to study the isolated phases, as well as in situ, the connected phases. It is of importance to note, that while the overall thermodynamic C_p and its integral functions of H, S, and G give mainly average results, the analysis of the glass transition, can yield information on the change of structure across the phase.

4. Multi-component nanophases

Molecules containing more than one incompatible component of sufficient size will nanophase separate within their crystals or mesophases. Fig. 19 illustrates the crystal structure of 4-*n*-octyloxybenzoic acid $CH_3{-}(CH_2{-})_7{-}O{-}C_6H_4{-}CO{-}OH$. If the octyl radicals were not chemically bound to the oxybenzoic acid radicals, both parts would fully phase separate. Being connected, they crystallize in the shown layer structure [72]. To make up for the different volume requirements, the aliphatic chains interdigitate and the final space adjustment is achieved by the monoclinic tilt. The flexible spacer is ca. 2.0 nm thick, a typical nanophase dimension [15].

Similar layer structures are known to exist for homopolymers with alkane side-chains of proper length [16 (vol. 3)], as well as precisely structured copolymers with sufficiently long alkane sequences [73]. In case the second component is too short or irregular to form its own nanophase, it remains amorphous in form of planes of intracrystalline defects. With sufficient decoupling at the connections to the crystalline alkane segments, the observed melting temperatures are close to those of paraffins with similar lengths [16,73].

Special nanophase structures were found in the nylons. In their crystals, the hydrogen bonds are located in intermolecular planes. Above the glass transition of the alkane sequences, the H-bonds keep the mobile CH_2-sequences in a parallel array. The liquid-like motion within the crystal is caused by conformational motion similar to the defect generation illustrated in Fig. 8 and does not affect the H-bonding significantly. In most nylons, the glass transition of the alkane sequences is accompanied by an expansion of the triclinic crystal without change in structure, i.e., one observes a glass transition of the crystal. In higher-melting nylons, T_g is linked to a transition to a pseudo-hexagonal mesophase structure, known as the Brill transition [74].

Interspersed semiflexible, aromatic mesogens within alkanes as are found, for example, in poly[oxy(3-methyl-1,4-phenylene)ethylene-1,4-phenyleneoxynonamethylene], MBPE-9, and lead to a nanophase separation. Such segmented polymers may display only partial conformational order. The chosen example has been analyzed by calorimetry, X-ray diffraction, and solid-state NMR [75–77]. The order in MBPE-9 involves identifiable CH_2 groups within the nonane sequences. Fig. 20 displays the heat capacity in the transition region. On heating, the heat capacity is already that of the liquid when the beginning of the disordering peak is reached, a common observation with mesophases. The lowest-temperature glass transition is that of the bulk-amorphous fraction of the MBPE-9 (40%), while the highest T_g corresponds to the condis-crystalline phase (43%, calculated from the heat of transition). The remaining MBPE-9 is assigned to a RAF (17%) and has a T_g located between the bulk-amorphous and condis phase.

As a last topic, the glass transition is analyzed in more detail to gain information about the properties throughout the microphases and nanophases. As the incompatible sequences in block-copolymers get longer, a phase-separation into microphases

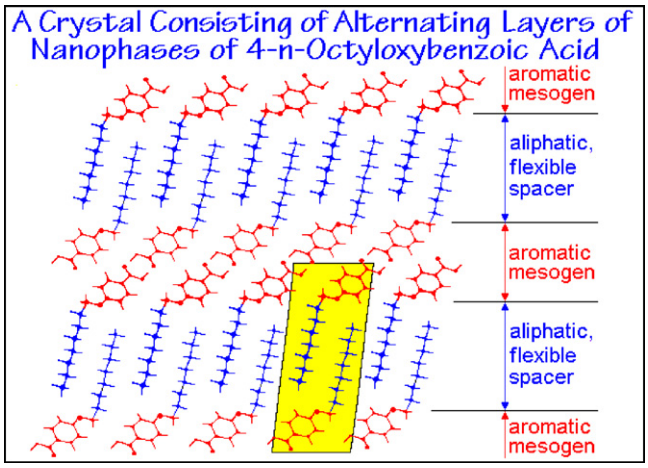

Fig. 19. Layer structure of alternating aliphatic and aromatic nanophases [82]. The unit cell, covering both layers, is marked at the bottom.

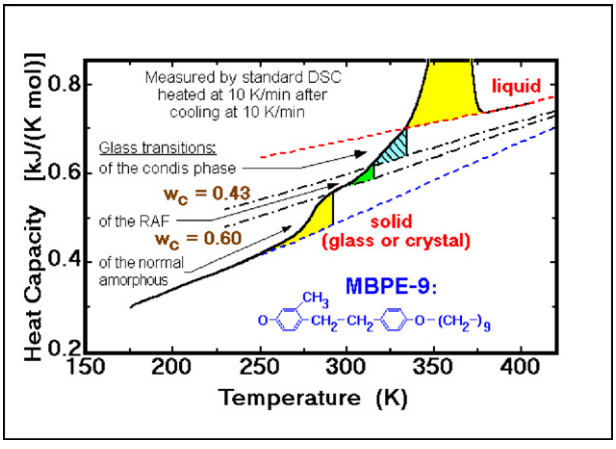

Fig. 20. The three glass transitions in poly[oxy(3-methyl-1,4-phenylene)ethylene-1,4-phenyleneoxynonamethylene], MBPE-9 [77]. The dashed-lines indicate the C_p of the solid (calculated from the vibrational spectrum fitted to low-temperature heat capacity) and the measured and extrapolated C_p of the liquid state. The two dash-dotted lines are calculated for the indicated crystallinities, w_c, and match the heat of transition ($w_c = 0.43$) and the lowest glass transition ($w_c = 0.60$) [77].

Please cite this article in press as: B. Wunderlich, Thermodynamics and properties of nanophases, Thermochim. Acta (2008), doi:10.1016/j.tca.2008.10.026

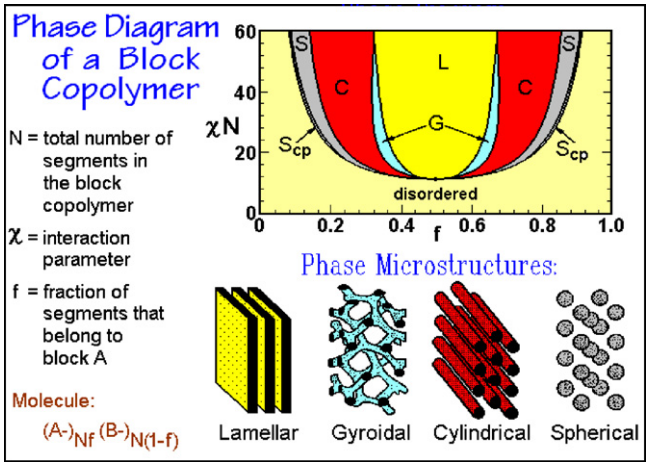

Fig. 21. Microphase separation in block copolymers. Depending on the concentration f and length of the segments, N, different self-assembly takes place [78]. The narrow phase area S_{cp} corresponds to a body-centered cubic arrangement.

takes place by a so-called self-organization. Fig. 21 shows the typical phase diagram [78], computed using the self-consistent mean-field theory. The various microphase structures are listed at the bottom of the figure. The interactions due to the lateral contacts between the sequences of A and B are represented by the Flory–Huggins parameter χN. The positive values of the abscissa indicate unfavorable free energy for the contacts between A and B, favoring phase separation. For the short sequences (small N) or low concentrations (f close to 0 or 1), the positive free energy of mixing can be compensated by the entropy of mixing, favoring formation of a solution (bottom and side portions of the diagram). Nanophase separation, thus, is expected only for molecules with a proper $N\chi$ and f.

The change of the glass transition on introducing a second component without change in chain-length distribution is illustrated in Fig. 22. A poly(oxy-2,6 dimethyl-1,4-phenylene) homopolymer is brominated on the position indicated in the structural formulae. The glass transition is moving to higher temperatures on the introduction of bromine radicals. Inspecting the breadth of the transition indicates no major change. The bromination does produced a random, single-phase, bulk copolymer [79].

Next, in solutions of a copolymer, the repeating units along the chain are fixed by the prior synthesis and cannot be randomized by the dissolution. Fig. 23A illustrates the glass transitions of a soluble pair of polymers, polystyrene, PS, and poly-α-methylstyrene, PMS [80]. As expected, with changing concentration, the T_g moves from

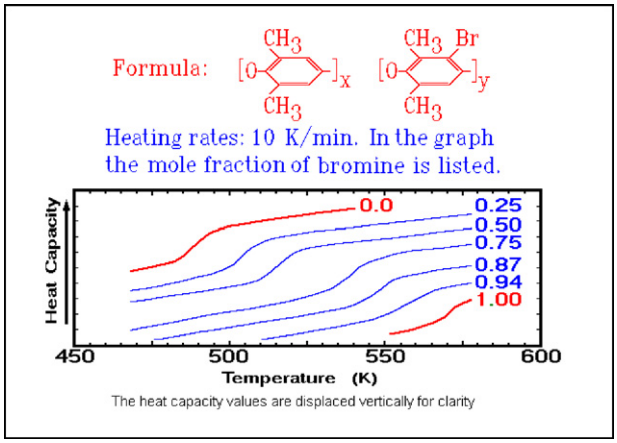

Fig. 22. The change in glass transition on increasing bromination of poly(oxy-2,6-dimethylphenylene) [79].

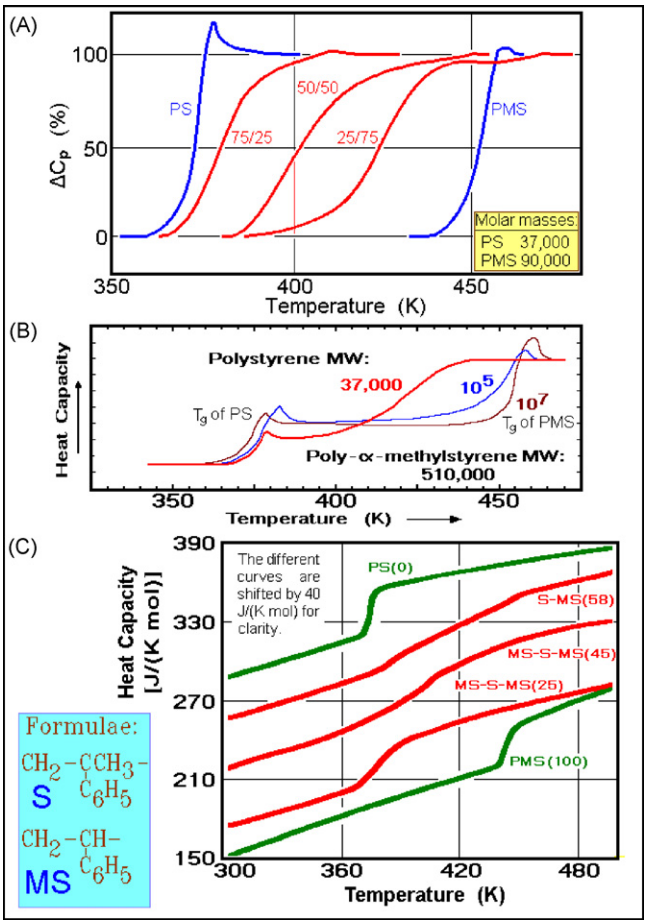

Fig. 23. Glass transitions and phase separations of polymer solutions of different molar masses (A and B) [80], and di- and tri-block copolymers of polysyrene, PS, and poly-α-methylstyrene, PMS (C) [67]. All concentrations are given in wt.%.

that of one homopolymer to that of the other homopolymer. What is not immediately obvious, is the reason for the large increase in the breadth of the transition range from 7 K for the pure polymers to 33 K for the solutions when measured by the tangent through T_g. Inspecting the shapes of the heat capacity shows a broadening in both temperature directions, in contrast to the crystallinity effect which causes an asymmetric broadening to higher temperature only (see Fig. 15) and for free-surface spheres which yield broadening to low temperature only (see Fig. 17). The minor component seems to broaden the transition most. Since the volume affecting the glass transition is small, one must assume that the inability to randomize the repeating units along the backbone atoms causes the broadening by producing clusters of unmixed components (nanophases?). Fig. 23B shows the changes when increasing the PMS molar mass in the blends by a factor 5.7 which reduces the solubility. Data are given for the various 50/50 wt.% concentrations of different molar masses of PS [80]. The 37,000 Da PS blend consists now of some phase-separated homopolymer PS and a solution PS/PMS with an intermediate T_g and a broadened transition range. Increasing the molar mass of the PS completes the phase separation. Details about the phase structure can be quantitatively read from the DSC traces. The results of a final series of blending is depicted in Fig. 23C, using di- and tri-block copolymers of the given concentrations and overall molar masses from 5×10^5 to 1×10^6 Da, i.e., the range of little solubility of the homopolymer sequences [68]. Indeed, the samples showed lamellar microphase separation of 45–120 nm when measured by electron microscopy [81]. The glass transitions are now spread over the whole temperature range set by the homopolymers, i.e., the glass transition of the

Please cite this article in press as: B. Wunderlich, Thermodynamics and properties of nanophases, Thermochim. Acta (2008), doi:10.1016/j.tca.2008.10.026

PS sequences in the microphase-separated block copolymers are now broadened to higher temperatures, and the glass transition of the PMS sequences is broadened to lower temperatures. The glass transition temperature, thus, is a sensitive tool to trace coupling across nanophase interfaces.

Other examples of such microphase separation with possible formation of nanaophases are available, but analyzed in less detail. The obvious tool for the nano-phase analysis is the quantitative calorimetry assessing time scales ranging from days to picoseconds, to be added to structure information. The microphases created by blending and synthesis of block copolymers are sufficiently large to allow additional internal phase separation in a smaller scale. For example, the di-block poly(oxyethylene-*block*-styrene) of molar masses 8.7 and 9.2 kDa, respectively, forms a melt macrophase solution down to 433 K. There, it self-assembles into a lamellar microphase of 18.7 nm spacing. Below 335 K, the polystyrene blocks become glassy, and below 324 K the poly(oxyethylene) blocks are semicrystalline. Since the spacing is close to the fold-length, the orientation of the crystals and their lateral perfection is strongly crystallization-temperature dependent [82]. Both the crystals and the intercrystalline amorphous chain segments in the poly(ethylene) lamellae may easily reach nanophase dimensions.

Poly[oligo(imino-1-oxododecamethylene)-*alt*-oligo(oxytetramethylene)]s which have been probed by DSC and TMDSC (commercial Pebax®) are another example [83]. In this case the block lengths were varied from 5 to 40 nm for the oligoamide segments and from 17 to 3 nm for the oligoether segments. The expected lamellar superstructure can be semicrystalline in each set of lamellae, producing rather complicated microphase and nanophase relationships. The melting points of all crystals were reduced from those of the homopolymers. The crystallinity of the oligoamide was increased for the longer segments due to a softening across the interface to the oligoethers with a lower glass transition, and the reverse is true for the oligoethers.

It is of interest to note that this important analysis of nanophases via calorimetry through the glass transition region applies also to poly(amino acid)s (nylon 2), the basic molecular sequences of proteins. The calorimetry of proteins is still in its very beginning [84] and nanophase glasses have not been analyzed as to their place in the hierarchy of chemical and physical structural ordering, although for some poly(amino acid)s, glass transitions are likely at reasonably low temperatures [85].

5. Conclusions

In the 21st century, nanophase science developed to a major focus in physics, chemistry, materials engineering, pharmacy, medicine, and biology. For a more precise definition, detailed in the present paper, the absence of recognizable bulk phase is required to identify a difference between microphases and nanophases [15]. Without this definition being widely accepted, many microphases have in the past been called nanophases, just because they fall into an arbitrarily picked size range. In many countries of the world, nanostructure analysis is by far the field of academic research with most governmental financial support. Without a clear definition, however, much of this support may be going to the long known and better understood microphase analysis, and progress toward the proposed goal, is thereby delayed.

From the first recognition of the large field of research on small particles of matter, some 50 years ago, it has been recognized that nanophases should have different properties than macrophases and microphases [1]. Today, the National Nanotechnology Initiative of the US in its popular science banner "Nano What??" states that: "Materials can have different properties at the nanoscale—some are better at conducting electricity or heat, some are stronger, some have different magnetic properties, and some reflect light better or change colors as their size changes [86]." The present review of the thermodynamics of nanophases asks of this statement only to be changed from "*can have different properties*" to the more definitive: "*must have different properties*." Naturally, one should also consider that many nanophases are less suited for a given task than microphases or even macrophases. Finally, in the light of the definition in Section 2, one may conclude that if there is no change in property, the matter researched, perhaps, is not a nanophase!

Overall, the novel ideas in the present paper can be summarized in five statements:

1. Nanophases fit into the general scheme of the molecules and phases.
2. There is a thermodynamic reason for the different crystal structures of nanophases.
3. Nanophases are not uniform throughout.
4. Macromolecules may be longer than the nanophases they are part of.
5. Segments of a macromolecule may be part of several different nanophases.

Point 1 was derived in Section 2 after the short history given in Section 1. In Sections 3 and 4 it was shown that nanophases are of importance for the description of a wide variety, if not all, of the chemical compounds.

Point 2 was suggested by the molecular dynamics simulations in Figs. 11 and 12 and the calorimetric evidence on Al_2O_3, TiO_2, and ZnS [55,56]. Similarly, a different growth mechanism was shown possible involving nanoparticles instead of atomic, small molecules, or sub-molecular units which are involved in the common crystal growth or Ostwald ripening [56].

Point 3 may be hardest to deal with when trying to arrive at a nanothermodynamics. Besides by molecular dynamics simulations, this change of properties from the surface to the center of a nanophase without reaching bulk properties has been demonstrated by the broadening of the glass transition. The glass transition is particularly well suited for nanophase analyses since the freezing of the long-range motion at T_g affects volumes of as little as 2 nm^3 or less, as seen from Fig. 8, and supported by the analysis of data on polystyrene [36]. Based on the observed broadening of the glass transition, a mean-field approach for the description of nanophases, as attempted in [8–10,46], seems of limited value.

Points 4 and 5 deal with flexible, linear macromolecules as represented by synthetic polymers, proteins, carbohydrates, and nucleic acids. It was emphasized that the molecules are uniquely longer than the nanophase dimensions. This leads to the coupling between neighboring phases at rotatable covalent bonds in the interface. This is not only a central issue for synthetic polymers, as analyzed for a number of molecules [65], but also for the flexible macromolecules of biological systems barely analyzed in this fashion [84,85].

A broader experimental base via nanophase calorimetry, as discussed in this 10th Lähnwitz Seminar, will help to develop a better understanding of "Thermodynamics and Properties of Nanophases" and connect the many, often seemingly random initial efforts. The hope expressed at the turn of the century that direct calorimetry on isolated nanophases may become possible [87], and the recently made progress to reduce the time scale of calorimetric measurements in the direction of the important picosecond frame for the large-amplitude molecular motion (along with the coupled decrease in sample mass) may become a key developments toward this experimental base for a nanothermodynamics [88].

References

[1] http://www.its.caltech.edu/~feynman/plenty.html.

Please cite this article in press as: B. Wunderlich, Thermodynamics and properties of nanophases, Thermochim. Acta (2008), doi:10.1016/j.tca.2008.10.026

[2] SciFinder™ (American Chemical Society) retrieves information produced by the Chemical Abstracts Service (CAS) as well as the MEDLINE® databases of the National Library of medicine (NML): http://www.cas.org./SCIFINDER.
[3] N. Taniguchi, Tokyo Sci. Univ., Noda, Japan, Kinzoku Hyomen Gijutsu 29 (1978) 220.
[4] Merriam Webster's Collegiate Dictionary, 11th edition, Merriam–Webster, Inc., Springfield, MA, 2003, see also: http://www.m-w.com/.
[5] H. Kopf, R.K. Joshi, M. Soliva, P. Speiser, Pharmazeutische Industrie 38 (1976) 281.
[6] J.P. Loreau, Sciences de la Terre 18 (3) (1973) 213.
[7] K.E. Gonsalves, P.R. Strutt, T.D. Xiao, P.G. Klemens, Polym. Preprints (ACS Div. Polym. Chem.) 32 (3) (1991) 559.
[8] T.L. Hill, Nano Lett. 1 (2001) 111.
[9] T.L. Hill, J. Chem. Phys. 36 (1962) 3182.
[10] T.L. Hill, Thermodynamics of Small Systems, Parts I and II, Benjamin, New York, 1963, 1964 (Refs. [9] and [10] were reprinted under the original title by Dover, New York, 1994).
[11] R.V. Chamberlin, Nature (Lond.) 408 (2000) 337.
[12] H.-F. Eicke, Surfact. Sci. Ser. 21 (1987) 41.
[13] Z. Li, S. Ramasamy, H. Hahn, R.W. Siegel, Mater. Lett. 6 (7) (1988) 195.
[14] K.H. Storks, J. Am. Chem. Soc. 60 (1938) 1753.
[15] W. Chen, B. Wunderlich, Macromol. Chem. Phys. 200 (1999) 283.
[16] B. Wunderlich, Macromolecular Physics, vol. 1–3, Academic Press, New York, 1973–1980 (A pdf reprint of with a new Preface and an electronically searchable index has been published in 2005 and is available via the European Virtual Institute for Thermal Metrology at their web site: http://www.evitherm.org/index.asp).
[17] For a summary of these topics see B. Wunderlich, Thermochim. Acta 340/41 (1999) 37.
[18] B. Wunderlich, M. Möller, J. Grebowicz, H. Baur, Conformational Motion and Disorder in Low and High Molecular Mass Crystals, Springer Verlag, Berlin (Adv. Polymer Sci. 87), 1988.
[19] B. Wunderlich, Int. J. Thermophys. 28 (2007) 958.
[20] http://www.ictac.org/.
[21] See, for example, B. Wunderlich, Thermal Analysis of Polymeric Materials, Springer-Verlag, Berlin, 2005, ISBN 978-3-540-23629-0 (Print), 978-3-540-26360-9 (Online), see also the detailed Computer Course: Thermal Analysis of Materials, available through http://athas.prz.rzeszow.pl and http://www.evitherm.org/index.asp.
[22] J. Dalton, "A New System of Chemical Philosophy." London, 1808; the ideas appeared first in his notebook covering 1802/04. Frequently reprinted; for example, see "The Science Classical Library", The Citadel Press, New York, 1964.
[23] W. Friedrich, P. Knipping, M. von Laue, Ann. Phys. 41 (1913) 971.
[24] The term "macromolecule was first used by H. Staudinger, J. Fritschi, Helv. Chim. Acta 5 (1922) 788; for the Nobel Lecture in 1953, see H. Staudinger, Arbeitserinnerungen, Hüthig Verlag, Heidelberg, Germany, 1961, p. 317, 312.
[25] The operational definition is discussed by P.W. Bridgeman, The Logic of Modern Physics, MacMillan, New York, 1927.
[26] B. Wunderlich, J. Therm. Anal. Calorim. 89 (2007) 321, ISSN 1572-8943 (Online).
[27] The importance of the glass transition is summarized in B. Wunderlich, Thermochim. Acta 446 (2006) 128; B. Wunderlich, J. Appl. Polym. Sci. 105 (2007) 49.
[28] B. Wunderlich, J. Grebowicz, Adv. Polym. Sci. 60/61 (1984) 1.
[29] For a detailed review see G.W. Gray, P.A. Winsor (Eds.), Liquid Crystals and Plastic Crystals, Wiley, Chichester, England, 1974; conformationally disordered (condis) crystals were suggested to exist in 1975 by G.W. Smith, in: G.H. Brown (Ed.), Advances in Liquid Crystals, vol. 1, Academic Press, New York, 1975, p. 193, and were documented with many examples [28,18].
[30] M.G. Friedel, Les Etats Mésomorphes de la Matiére, Ann. Phys. (Paris) 18 (1922) 273.
[31] P. Ehrenfest, Phase changes in the ordinary and extended sense classified according to the corresponding singularities of the thermodynamic potential, Proc. Acad. Sci., Amsterdam 36 (1933) 153–157 (Suppl. 75b, Mitt Kammerlingh Onnes Inst, Leiden).
[32] J.W. Gibbs, Trans. Conn. Acad. III (1875) 108; an extended abstract was published in: Am. J. Science, Ser. 3, 16 (1878) 441. Reprinted in H.A. Bumstead, R. Gibbs van Name, The Scientific Papers of J. Willard Gibbs, vol. 1, Thermodynamics, Dover Publ., New York, 1961 and later.
[33] M. Pyda, http://athas.prz.rzeszow.pl.
[34] For an early discussion see G. Tammann, Z. anorg. allg. Chemie 111 (1920) 166; R.C. Tolman, J. Chem. Phys. 16 (1948) 758.
[35] For early experiments see F. Meissner, Z. anorg. allg. Chemie 111 (1920) 169.
[36] The hole theory of liquids [H. Eyring, J. Chem. Phys. 4 (1936) 283] was applied to the glass transition by N. Hirai, H. Eyring, J. Appl. Phys. 29 (1958) 810. The cited size-evaluation and energy of holes in polystyrene: B. Wunderlich, D.M. Bodily, M.H. Kaplan, J. Appl. Phys. 35 (1964) 95.
[37] Liquids lead to spherical droplets if not distorted by gravity, and for crystals, the shape of minimal surface free energy is fixed by the so-called Wulff-construction G. Wulff, Z. Krist. 34 (1901) 449.
[38] M. Faraday, Philos. Trans. R. Soc. (Lond.) 147 (1847) 145.
[39] For a recent review of iron nanoparticles see D.L. Huber, nano, 1 No. 5, Wiley-VCH, Weinheim, 2005, p. 482, www.small-journal.com.
[40] J.A. Morrison, L.E. Drain, J. Chem. Phys. 19 (1951) 1063.
[41] J.A. Morrison, J.M. Los, Faraday Soc. Discuss. 8 (1950) 321.
[42] S.N. Magonov, N.A. Yerina, G. Ungar, D.H. Reneker, D.A. Ivanov, Macromolecules 36 (2003) 5637.
[43] J. Pak, B. Wunderlich, Macromolecules 34 (2001) 4492.
[44] C.-Y. Ruan, Y. Murooka, R.K. Raman, R.A. Murdick, Nano Lett. 7 (2007) 1290.
[45] P. Buffat, J.P. Borel, Phys. Rev. A 13 (1976) 2287.
[46] C.X. Wang, G.W. Yang, Mater. Sci. Eng. R 49 (2005) 157.
[47] B.G. Sumpter, D.W. Noid, G.L. Liang, B. Wunderlich, Atomistic dynamics of macromolecular crystals, Adv. Polym. Sci. 116 (1994) 27–72 (Vol. on "Atomistic Modeling of Physical Properties of Polymers" Eds. U. Suter, L. Monnerie).
[48] B. Wunderlich, M. Pyda, J. Pak, R. Androsch, Thermochim. Acta 377 (2001) 9.
[49] Y. Kim, H.L. Strauss, R.G. Snyder, J. Phys. Chem. 93 (1989) 7520.
[50] S.N. Kreitmeier, G.L. Liang, D.W. Noid, B. Wunderlich, Polym. Int. 36 (1995) 155.
[51] G.L. Liang, D.W. Noid, B.G. Sumpter, B. Wunderlich, J. Comp. Polym. Sci. 3 (1993) 101.
[52] A.I. Kitaigorodskii, Organicheskaya Kristallokhimiya, Acad. Sci. USSR: Moscow (1955) (Chemical Organic Crystallography, English Translation, Consultants Bureau: New York, 1961); and Molecular Crystals and Molecules, Academic Press, New York, 1973.
[53] G.L. Liang, D.W. Noid, B.G. Sumpter, B. Wunderlich, Acta Polymerica 44 (1993) 214.
[54] See, for example the reviews H. Gleiter, Nanostruct. Mater. 6 (1995) 3; W. Siegel, Nanostruct. Mater. 4 (1994) 121.
[55] Following the discussion by J.M. McHale, A. Auroux, A.J. Perrotta, A. Navrotsky, Science 277 (1997) 788.
[56] As described in a review by B. Gilbert, H. Zhang, F. Huang, M.P. Finnegan, G.A. Waychunas, J.F. Banfield, Geochem. Trans. 4 (2003) 20.
[57] R. Festag, S.D. Alexandratos, K.D. Cook, D.C. Joy, B. Annis, B. Wunderlich, Macromolecules 30 (1997) 6238.
[58] D.H. Reneker, I. Chun, Nanotechnology 7 (1996) 216.
[59] C. Huang, S. Chen, C. Lai, D.H. Reneker, H. Qiu, Y. Ye, H. Hou, Nanotechnology 17 (2006) 1558.
[60] A. Mathur, J. Erlebacher, Appl. Phys. Lett. 90 (2007) 061910.
[61] H. Bu, Y. Pang, D. Song, T. Yu, T.M. Voll, G. Czornyj, B. Wunderlich, J. Polym. Sci., Part B. Polym. Phys. 29 (1991) 139.
[62] H. Bu, E. Chen, S. Xu, K. Guo, B. Wunderlich, J. Polym. Sci., Part B: Polym. Phys. 32 (1994) 1351.
[63] I. Okazaki, B. Wunderlich, J. Polym. Sci., Part B: Polym. Phys. 34 (1996) 2941.
[64] H. Suzuki, J. Grebowicz, B. Wunderlich, Br. Polym. J. 17 (1985) 1.
[65] B. Wunderlich, Prog. Polym. Sci. 28/3 (2003) 383.
[66] M. Kunz, M. Möller, U.-R. Heinrich, H.-J. Cantow, Makromol. Chem. Symposia 20/21 (1988) 147;
M. Kunz, M. Möller, U.-R. Heinrich, H.-J. Cantow, Makromol. Chem. Symposia 23 (1989) 57.
[67] M. Pyda, E. Nowak-Pyda, J. Heeg, H. Huth, A.A. Minakov, M.L. Di Lorenzo, C. Schick, B. Wunderlich, J. Polym. Sci., Part B: Polym. Phys. 44 (2006) 1364.
[68] U. Gaur, B. Wunderlich, Macromolecules 13 (1980) 1618.
[69] B. Wunderlich, Thermochim. Acta 403 (2003) 1.
[70] A. Miyagi, B. Wunderlich, J. Polym. Sci., Polym. Phys. Ed. 10 (1972 2073).
[71] O.A. Battista, Microcrystal Polymer Science, McGraw-Hill, New York, 1975.
[72] R.F. Bryan, P. Hartley, R.W. Miller, M.-S. Shen, Mol. Cryst. Liq. Cryst. 62 (1980) 281.
[73] W. Qiu, J. Sworen, M. Pyda, E. Nowak-Pyda, A. Habenschuss, K.B. Wagener, B. Wunderlich, Macromolecules 39 (2006) 204.
[74] B. Wunderlich, J. Therm. Anal. Calorim. 93 (2008) 7.
[75] M.A. Yandrasits, S.Z.D. Cheng, A. Zhang, J. Cheng, B. Wunderlich, V. Percec, Macromolecules 25 (1992) 2112.
[76] J. Cheng, Y. Jin, B. Wunderlich, S.Z.D. Cheng, M.A. Yandrasits, A. Zhang, V. Percec, Macromolecules 25 (1992) 5991.
[77] Y. Jin, J. Cheng, B. Wunderlich, S.Z.D. Cheng, M.A. Yandrasits, Polym. Adv. Technol. 5 (1994) 785.
[78] M.W. Matsen, F.S. Bates, Macromolecules 29 (1996) 1091;
M.W. Matsen, F.S. Bates, J. Chem. Phys. 106 (1997) 2436.
[79] R.C. Bopp, U. Gaur, R.P. Kambour, B. Wunderlich, J. Therm. Anal. 25 (1982) 243.
[80] S.-F. Lau, J. Pathak, B. Wunderlich, Macromolecules 15 (1982) 1278.
[81] S. Krause, D.J. Dunn, A. Seyed-Mozzafari, A.M. Biswas, Macromolecules 10 (1977) 786.
[82] L. Zhu, S.Z.D. Cheng, S.L. Thomas, B. Lotz, J. Am. Chem. Soc. 122 (2000) 5957.
[83] M.L. Di Lorenzo, M. Pyda, B. Wunderlich, J. Polym. Sci., Part B: Polym. Phys. 39 (2001), 1594, 2969.
[84] The basic heat capacity measurements on solid, water-free polyamids, copolyamids, and proteins and their analysis relative to vibrational contributions are available in: K.A. Roles, B. Wunderlich, Biopolymers 31 (1991) 477; K.A. Roles, A. Xenopoulos, B. Wunderlich, Biopolymers 33 (1993) 753; J. Polym. Sci., Part B: Polym. Phys. 31 (1993) 279; G. Zhang, B.V. Lebedev, B. Wunderlich, J.-Y. Zhang, J. Polym. Sci., Part B: Polym. Phys. 33 (1995) 2449; G. Zhang, S. Gerdes, B. Wunderlich, Macromol. Chem. Phys. 197 (1996) 3791; G. Zhang, B. Wunderlich, J. Therm. Anal. 49 (1997) 823.
[85] A. Xenopoulos, K.A. Roles, B. Wunderlich, Polymer 34 (1993) 2559.
[86] http://www.nano.gov/Nanotechnology_BigThingsfromaTinyWorld.pdf.
[87] B. Wunderlich, Thermochim. Acta 355 (2000) 43.
[88] For superfast calorimetry see, for example, the proceedings of the 8th and 9th Lähnwitz Seminars, Thermochim. Acta 432 (2005); 461 (2007).

Please cite this article in press as: B. Wunderlich, Thermodynamics and properties of nanophases, Thermochim. Acta (2008), doi:10.1016/j.tca.2008.10.026